NASA TECHNICAL MEMORANDUM

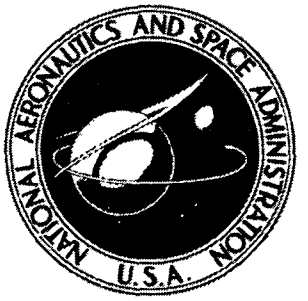

NASA TM X-2615

NASA TM X-2615

OXYGEN-HYDROGEN INJECTOR PERFORMANCE AND COMPATIBILITY WITH ABLATIVE CHAMBERS

by John P. Wanhainen

Lewis Research Center

Cleveland, Ohio 44135

NATIONAL AERONAUTICS AND SPACE ADMINISTRATION • WASHINGTON, D. C. • SEPTEMBER 1972

1. Report No.	2. Government Accession No.	3. Recipient's Catalog No.
NASA TM X-2615		

4. Title and Subtitle	5. Report Date
OXYGEN-HYDROGEN INJECTOR PERFORMANCE AND COMPATIBILITY WITH ABLATIVE CHAMBERS	September 1972
	6. Performing Organization Code
7. Author(s)	8. Performing Organization Report No.
John P. Wanhainen	E-6926
	10. Work Unit No.
9. Performing Organization Name and Address	113-31
Lewis Research Center National Aeronautics and Space Administration Cleveland, Ohio 44135	11. Contract or Grant No.
	13. Type of Report and Period Covered
12. Sponsoring Agency Name and Address	Technical Memorandum
National Aeronautics and Space Administration Washington, D. C. 20546	14. Sponsoring Agency Code

15. Supplementary Notes

16. Abstract

An experimental investigation was conducted to develop a high-thrust, high-performance, concentric tube injector element for use with near liquid hydrogen and liquid oxygen propellants. A parallel tube coaxial injector yielded 98 percent theoretical characteristic exhaust velocity efficiency. Installation of swirlers in the oxidizer tube improved performance but caused high ablative erosion near the injector. Film cooling significantly reduced ablative erosion near the injector but did not completely alleviate gouging adjacent to each outer injection element.

17. Key Words (Suggested by Author(s))	18. Distribution Statement
Oxygen - hydrogen injector Ablative chambers Combustion performance	Unclassified - unlimited

19. Security Classif. (of this report)	20. Security Classif. (of this page)	21. No. of Pages	22. Price*
Unclassified	Unclassified	28	$3.00

* For sale by the National Technical Information Service, Springfield, Virginia 22151

OXYGEN-HYDROGEN INJECTOR PERFORMANCE AND COMPATIBILITY WITH ABLATIVE CHAMBERS

by John P. Wanhainen

Lewis Research Center

SUMMARY

An experimental investigation was conducted to develop a high-thrust, high-performance, concentric tube injector element for use with near liquid hydrogen and liquid oxygen propellants. Seven different element designs were evaluated. Each element design was tested in a 19-element, 13.68-centimeter- (5.39-in.-) diameter circular pattern injector. The design vacuum thrust per element at a chamber pressure of 3448 kilonewtons per square meter absolute (500 psia) was 2558 newtons (575 lb). In addition to the performance tests, a few tests were also conducted to check the injector-ablative chamber compatibility of two element designs.

A parallel tube coaxial injector designed for a hydrogen injection velocity of 158.5 meters per second (520 ft/sec) and an oxygen injection velocity of 12.2 meters per second (40 ft/sec) yielded 98 percent theoretical characteristic exhaust velocity efficiency. Installation of swirlers in the oxidizer tube improved performance but caused higher ablative erosion near the injector. Film cooling significantly reduced ablative erosion near the injector, but did not completely alleviate gouging adjacent to each outer injection element.

INTRODUCTION

In the interest of reducing vehicle costs and thereby reducing the cost per pound of payload in orbit, a task was undertaken at Lewis Research Center to develop technology for low-cost, hydrogen-oxygen booster engines. The task was primarily directed toward developing injector technology to allow the use of ablative materials which could be fabricated at low cost and which could be repaired or replaced in otherwise uncooled steel thrust chambers. With the proposed ablative cooling technique, the hydrogen would enter the injector at near liquid temperatures, a condition at which high combus-

tion efficiency has been difficult to obtain. The results of reference 1 have shown a severe dropoff in performance at low hydrogen temperatures with large thrust per element injectors. The effort presented herein was, therefore, undertaken to develop a high performance injector element from which a large-size, high-performance, uniform heat flux injector could be fabricated for use in the cooling technology program. However, due to manpower and funding limitations, the program was terminated after this small-scale performance and ablative compatibility study.

The tests reported herein were limited to concentric-tube injector elements, the type used almost exclusively with the hydrogen-oxygen propellant combination. The elements were typical of those used in large hydrogen-oxygen booster engines such as M-1. Each injector had 19 elements, and each element had a design propellant flow rate of 0.58 kilogram per second (1.3 lb/sec) for a nominal vacuum thrust per element of 2558 newtons (575 lb). The injector element designs investigated included (1) a parallel tube element, (2) a taper-reamed oxidizer tube element, (3) a recessed oxidizer tube element, (4) an oxidizer swirler element, (5) a castellated oxidizer tube element, (6) an impinging fuel element, and (7) a high hydrogen velocity element.

The tests to measure injector performance were of short duration and were conducted in 13.68-centimeter- (5.39-in.-) diameter graphite-lined combustors. The combustor which had a contraction ratio of 1.9 produced a sea level thrust of about 36 910 newtons (8300 lb) at a chamber pressure of 3448 kilonewtons per square meter absolute (500 psia). Performance was measured over a range of oxidant-fuel ratios from about 4 to 6. Hydrogen injection temperature was not intentionally changed; however, because a simple pressurized fuel system was used for the tests, the injection temperature varied from 30.5 to 38.9 K (55° to 70° R) for these tests due to varying amounts of heat transfer into the hydrogen from the propellant system.

In addition to the performance tests, a few tests to check injector influence on ablative erosion were conducted with the parallel-tube element and swirler element injectors. The thrust chambers used for the ablative erosion tests consisted of a stack of 2.54-centimeter- (1-in.-) long cylindrical rings fabricated from a paper-filled phenolic material with ablative qualities such that a measurable amount of erosion would occur in a total firing duration of 5 seconds.

APPARATUS

Test Facility

The Rocket Engine Test Facility (fig. 1) of the Lewis Research Center is a remotely operated, 222.5-kilonewton- (50 000-lb-) thrust sea level stand equipped with an exhaust gas muffler and scrubber. The engine was mounted on the thrust stand to fire

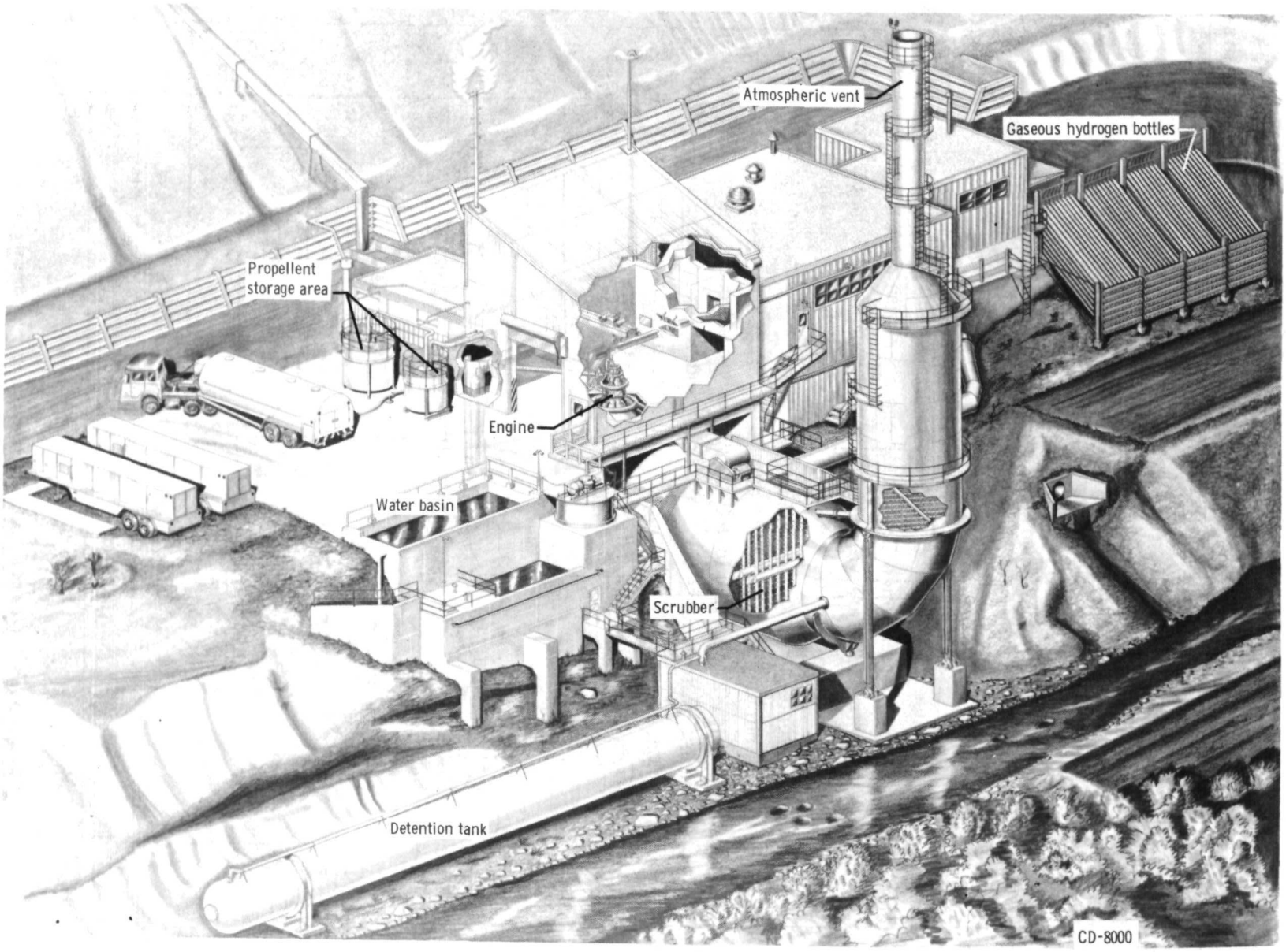

Figure 1. - Test facility.

vertically downward into the scrubber where the exhaust gases were sprayed with water for the purpose of cooling and sound suppression. The cooled exhaust gases were discharged into the atmosphere from the 21.33-meter- (70-ft-) high exhaust stack. The facility utilized a pressurized propellant system to deliver the propellants to the engine from the storage tanks. A more detailed description of the facility is given in reference 2.

Rocket Engine

The rocket engine used for the performance tests consisted of an injector with a removable faceplate, a cylindrical uncooled thrust chamber with a 13.68-centimeter (5.39-in.) inside diameter and a convergent-divergent, uncooled exhaust nozzle with a contraction ratio of 1.9 and an expansion ratio of 1.57. (The expansion ratio was selected for operating convenience since the tests were conducted in a sea level facility.) The length of the cylindrical section of the combustor was 38.1 centimeters (15 in.). The thrust chamber (fig. 2) was fabricated from heavy-wall carbon steel and utilized ATJ (or equivalent) graphite inserts for both the cylindrical section and the convergent-divergent exhaust nozzle. A seal of silicone rubber compound was provided on the end of the nozzle to prevent flow of combustion gases behind the inserts.

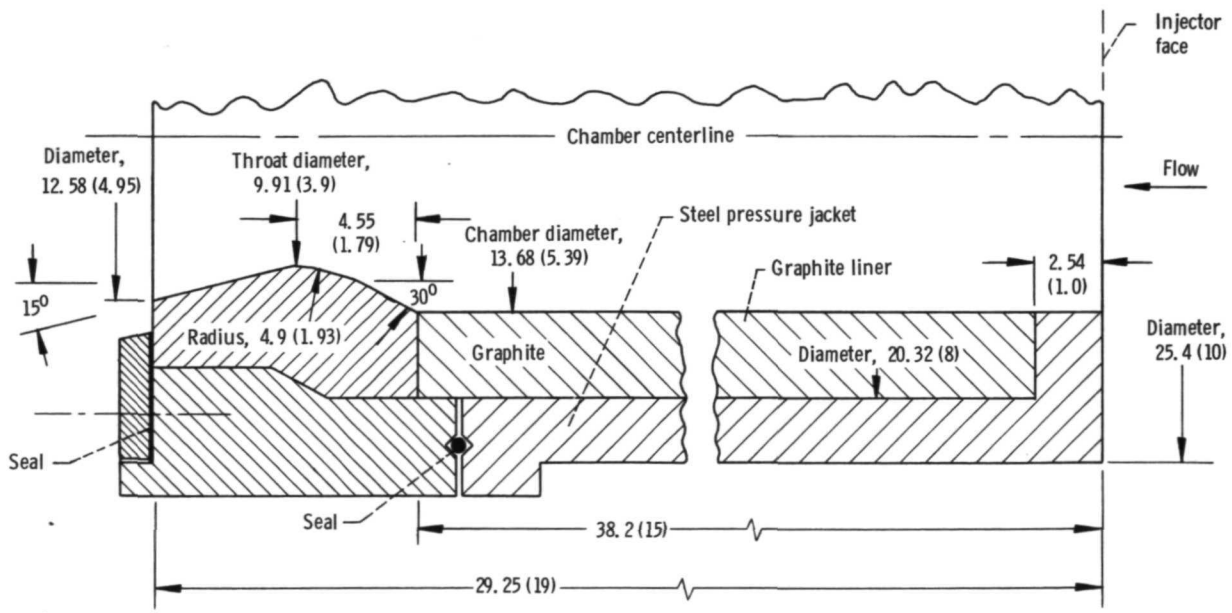

Figure 2. - Heavy wall steel with ATJ graphite liner thrust chamber. (All dimensions in cm (in.) unless indicated otherwise.)

For the ablative chamber erosion tests, the graphite liner in the cylindrical section of the thrust chamber was replaced with a stack of 2.54-centimeter- (1-in.-) long ablative cylindrical rings (fig. 3). When installed in the chamber, the rings were under a slight axial compressive load to prevent gaps and flow of combustion gases behind the ablative liner. The rings were fabricated from a paper-reinforced phenolic ablative, purposely selected for its high erosion qualities so that a measurable amount of erosion would occur in the 5-second total duration tests.

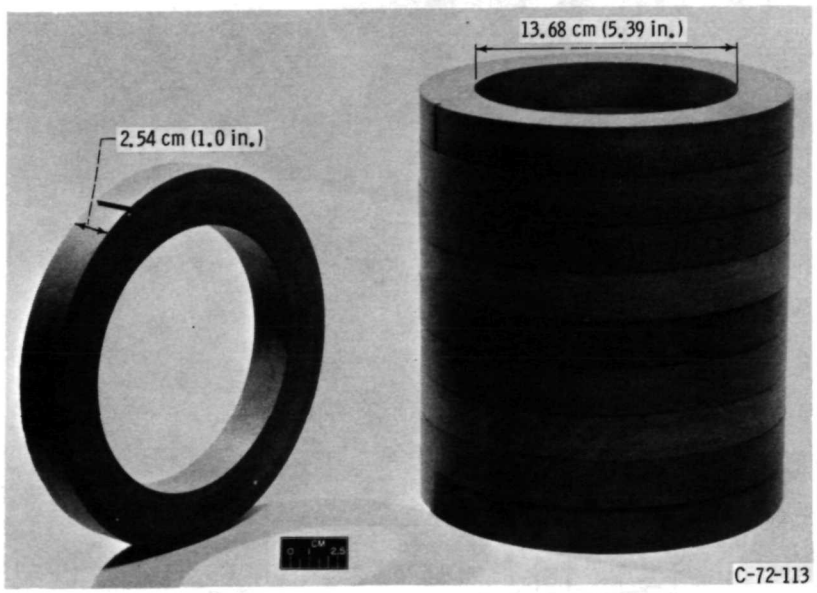

Figure 3. - Paper reinforced phenolic ablative thrust chamber inserts.

Measurement of erosion in the thrust chamber was greatly facilitated by the sectional thrust chamber. After a firing, the thrust chamber was disassembled, a paper tracing made of the inner diameter of each ring, and the tracing then planimetered to determine the cross-sectional area at 2.54-centimeter (1-in.) axial increments for the length of the chamber.

Faceplate and cross-sectional views of the 19-element concentric tube injector are shown in figure 4. The particular element pattern was selected for uniform radial and circumferential distribution. For ease of modification, both the elements and the injector faceplate were removable from the injector body. The oxidizer tube was screwed into the propellant distribution plate and could be removed without disturbing the fuel sleeve or faceplate. The faceplate was fabricated from 1.27-centimeter- (0.50-in.-) thick oxygen-free copper, a material with good heat-sink capability; thus, the need for careful attention to coolant-flow requirements within the injector was eliminated. As

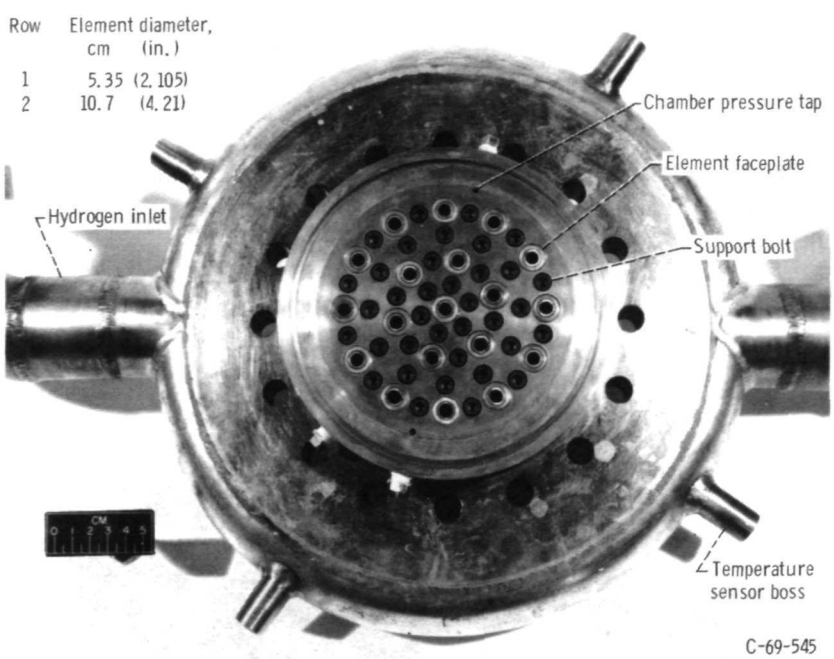

(a) Faceplate view.

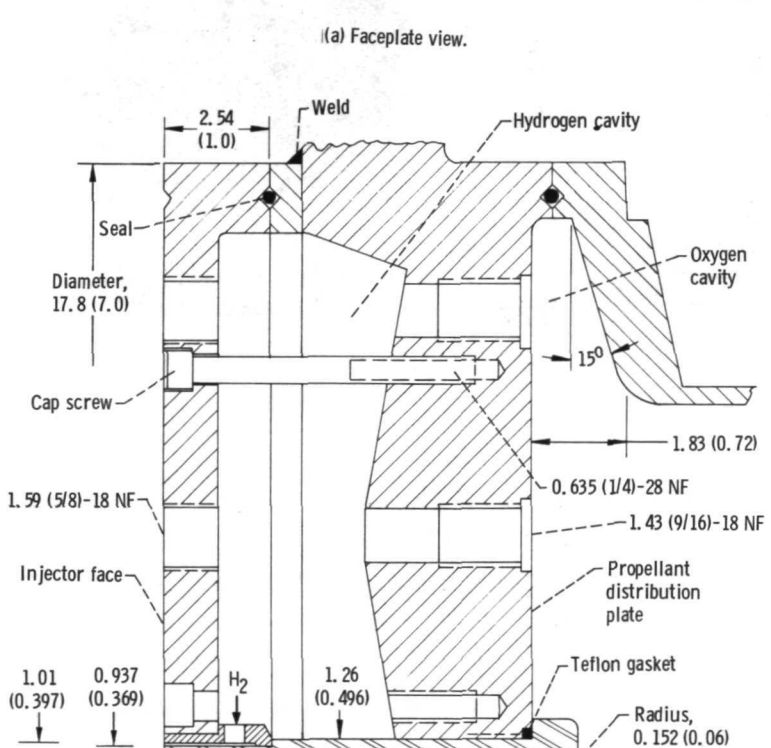

(b) Cross-sectional view. (All dimensions in cm (in.) unless indicated otherwise.

Figure 4. - Nineteen element concentric tube injector with removeable faceplate and elements.

will be discussed later, the baseline element (configuration 1) was designed for as high a hydrogen to oxygen injection velocity differential as considered pratical. A hydrogen injection pressure drop of 1724 kilonewtons per square meter (250 psi) was arbitrarily assumed to be the upper limit for a chamber pressure of 3448 kilonewtons per square meter absolute (500 psia). The design hydrogen injection area was 2.075 square centimeters (0.322 sq in.). Counterboring the oxidizer tube exit was utilized to provide a low injection velocity and yet maintain a high differential pressure for good chugging stability. For the baseline configuration, the oxygen flow metering and injection (tube exit) areas were 1.78 and 6.8 square centimeters (0.276 and 1.055 sq in.), respectively.

Cross-sectional views of all the elements tested are shown in figure 5. The configurations include a parallel tube element (fig. 5(a)), a taper-reamed oxidizer tube element (fig. 5(b)), a recessed oxidizer tube element (fig. 5(c)), an oxidizer swirler

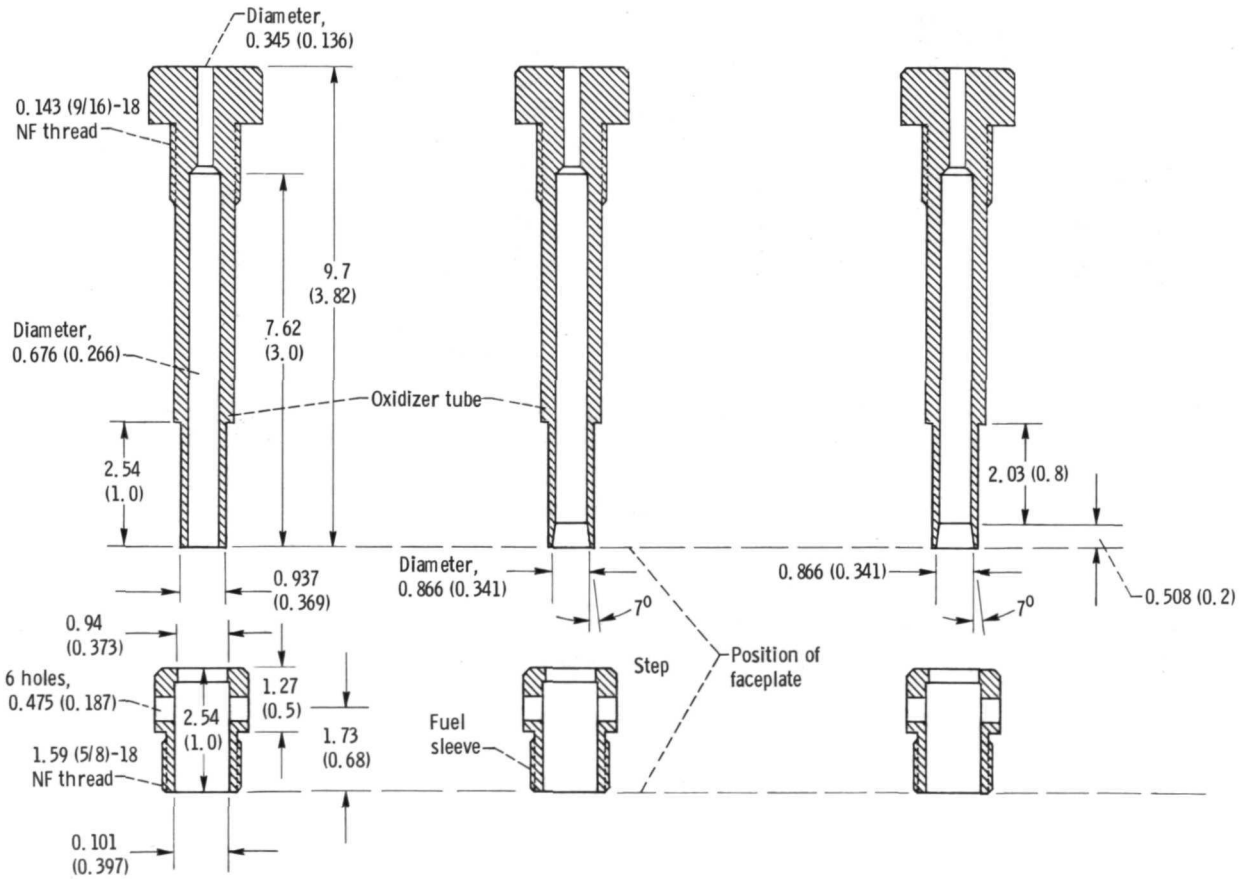

(a) Configuration 1 (parallel tube element).

(b) Configuration 2 (taper-reamed oxidizer tube element).

(c) Configuration 3 (recessed oxidizer tube element).

Figure 5. - Element configurations for 19-element injector. (All dimensions in cm (in.) unless indicated otherwise.)

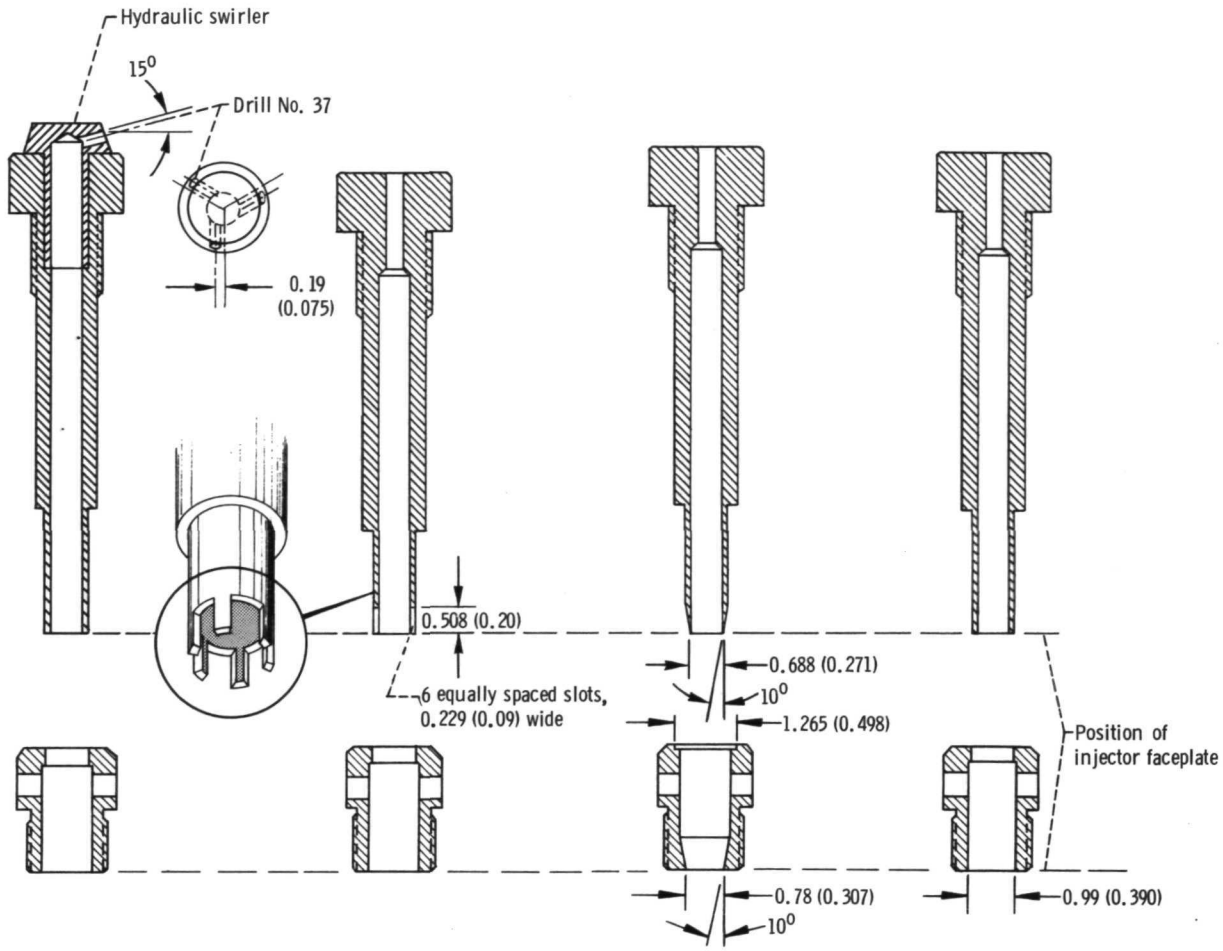

(d) Configuration 4 (oxidizer swirler element).

(e) Configuration 5 (castellated oxidizer tube element).

(f) Configuration 6 (impinging fuel element).

(g) Configuration 7 (high hydrogen velocity element).

Figure 5. - Concluded.

element (fig. 5(d)), a castellated oxidizer tube element (fig. 5(e)), an impinging fuel element (fig. 5(f)), and a high hydrogen velocity element (fig. 5(g)).

Instrumentation

The instrumentation used in the investigation and the location of the various transducers are shown in the diagram of the engine and propellant system in figure 6. The parameters were recorded on an automatic digital data recording system and as well as on direct reading instruments in the control room of the facility for monitoring during tests. Strain gage transducers were used to measure steady-state pressures. Propellant weight flows were determined with a turbine flowmeter in the case of the oxidizer

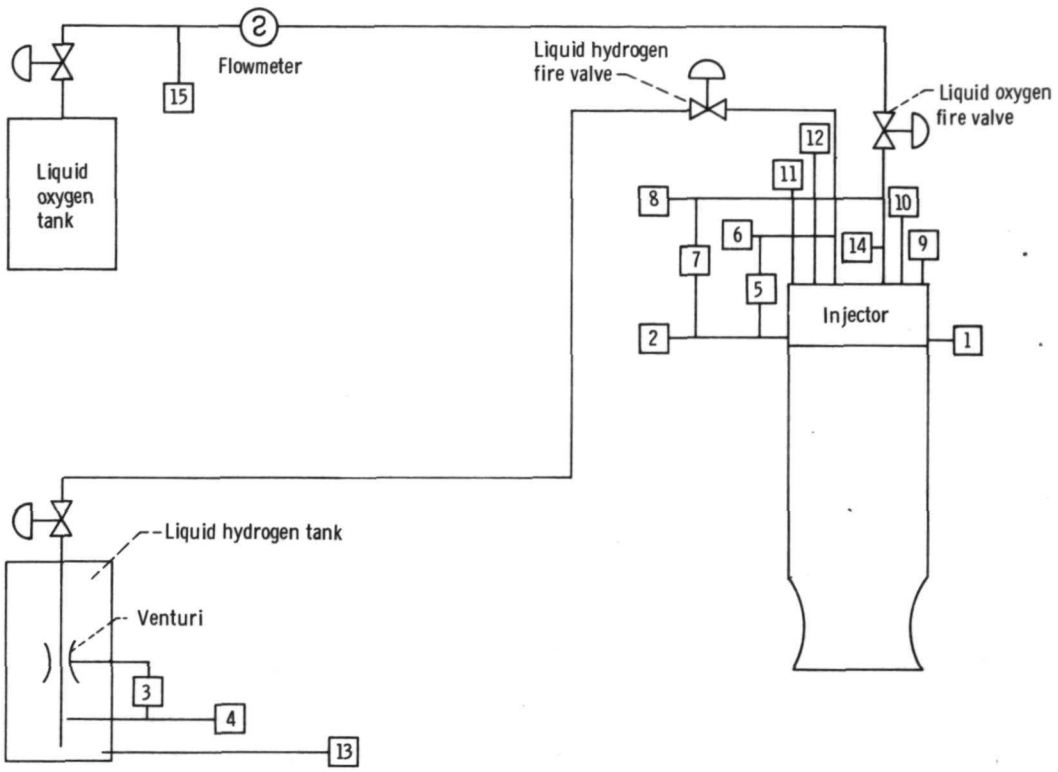

1 Static chamber pressure (injector face), four-arm strain-gage transducer 1
2 Static chamber pressure (injector face), four-arm strain-gage transducer 2
3 Liquid-hydrogen venturi differential pressure, four-arm strain-gage transducer
4 Liquid-hydrogen venturi pressure, four-arm strain-gage transducer
5 Hydrogen-injection differential pressure, four-arm strain-gage transducer
6 Hydrogen-injector pressure, four-arm strain-gage transducer
7 Oxygen-injection differential pressure, four-arm strain-gage transducer
8 Oxygen-injector pressure, four-arm strain-gage transducer
9 Hydrogen-injector temperature, carbon-resistor-sensor probe 1
10 Hydrogen-injector temperature, carbon-resistor-sensor probe 2
11 Hydrogen-injector temperature, carbon-resistor-sensor probe 3
12 Hydrogen-injector temperature, carbon-resistor-sensor probe 4
13 Liquid-hydrogen venturi temperature, platinum resistor sensor
14 Oxygen-injector temperature, copper-constantan thermocouple
15 Oxygen flowmeter temperature, platinum resistor sensor

Figure 6. - Instrumentation diagram.

and a venturi for the fuel. Platinum resistor sensors were used to measure propellant temperatures. All transducers used for recording steady-state data were calibrated immediately prior to data acquisition by an electrical two-step calibration system which used resistances in an electrical circuit to simulate a given full-scale reading.

A piezoelectric-type water-cooled pressure transducer was used on the thrust chamber to measure any high frequency pressure disturbances in the combustor. The signal from the high frequency transducer was recorded on magnetic tape, then replayed at reduced speed onto an oscillograph for analysis.

Procedure

Program timers were used to sequence the propellant valves. Starting about 2 seconds prior to the oxidizer valve opening. the hydrogen feed system was thermally conditioned by flowing a small amount of liquid hydrogen through the system and injector. The initial operating conditions were selected by presetting the fire valves. Approximately 1/2 second after the start signal, propellant flow rates were regulated by an electrohydraulic controller to maintain a given chamber pressure and oxidant-fuel ratio. The duration of the firings was short, usually about 2 seconds, to minimize nozzle throat erosion. The engine was inspected after each series of tests and the throat diameter was measured for performance calculations.

RESULTS AND DISCUSSION

The performance data presented were calculated from chamber pressure measurements corrected for momentum pressure losses (appendix A). Performance is presented in terms of characteristic velocity efficiency expressed as a percentage of the theoretical shifting equilibrium value from reference 3. The nominal operating conditions were a chamber pressure of 3448 kilonewtons per square meter absolute (500 psia) and oxidant-fuel ratios from 4 to 6.

Combustion Performance

Configuration 1 (parallel tube element). - For a baseline, a parallel tube element (fig. 5(a)) was designed based upon the author's experience with combustion of very cold gas hydrogen and liquid oxygen propellants. The results of a previous experiment (ref. 2) indicated that high performance could be maintained from warm gas to near

liquid hydrogen temperatures providing the hydrogen injection area was decreased (compensating for the change of density with temperature) to maintain a high injection velocity. High hydrogen injection velocity is also beneficial from the standpoint of acoustic mode stability margin (ref. 2). Based upon these results, the baseline element was designed for as high a hydrogen injection velocity as considered practical from an injector pressure drop standpoint. The injector differential pressure of 1724 kilonewtons per square meter (250 psi) at rated hydrogen flow was arbitrarily assumed to be the practical upper limit for a chamber pressure of 3448 kilonewtons per square meter absolute (500 psia). At a hydrogen injection temperature of 33.3 K (60° R), the injection velocity was about 158.5 meters per second (520 ft/sec).

The technique (ref. 2) of counterboring to provide a low oxygen exit velocity (for high differential injection velocity) and yet maintaining a high differential pressure for good chugging stability was used on the oxidizer tube. At rated conditions and an oxidant-fuel ratio of 5, the design injector oxygen pressure drop was 965 kilonewtons per square meter (140 psi) and the exit velocity computed using the tube exit area was 12.2 meters per second (40 ft/sec).

The performance of the baseline element in a 43.2-centimeter- (17-in.-) long combustor ($L^* \cong 76$ cm (30 in.)) is shown in figure 7 as a function of oxidant-fuel ratio. At an oxidant-fuel ratio of 5, the characteristic exhaust velocity efficiency was 98 percent. The standard deviation for these data was estimated at ±0.54 percent. Noted on the figure is the hydrogen injector inlet temperature which varied between 32.2 and 38.9 K (58° and 70° R) for these data. No trend with temperature is apparent in the data. The effect of oxidant-fuel ratio on performance appears minimal over the range tested; however, only a limited amount of data were taken at oxidant-fuel ratios other than 5. Although the performance and operating characteristics of the first configuration were satisfactory for use in the follow-on ablative cooling investigation, testing of various element designs was continued in an attempt to achieve even higher performance.

Configuration 2 (taper-reamed oxidizer tube element). - The first element modification (which consisted of taper-reaming all oxidizer tubes) was made to determine the

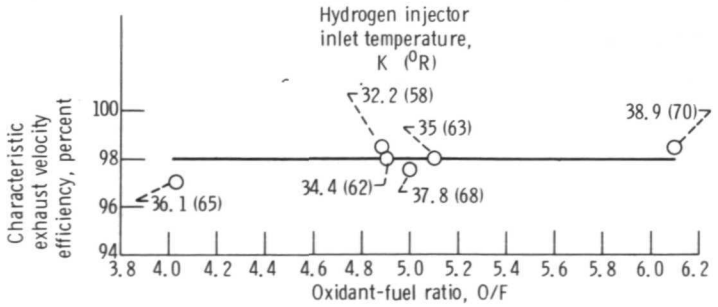

Figure 7. - Base line element performance. Nominal chamber pressure, 3448 kilonewtons per square meter absolute (500 psia).

effect of further reducing oxidizer injection velocity or increasing the residence time of the oxygen on combustion performance. Assuming that the element would flow full, the oxygen injection velocity was reduced from 12.2 (baseline element) to 7.32 meters per second (40 (baseline element) to 24 ft/sec).

The results obtained with this configuration and all other element configurations tested are compared in figure 8. Comparing the data of configuration 2 to the baseline indicates that a reduction in oxidizer injection velocity from 12.2 to 7.32 meters per second (40 to 24 ft/sec) had no significant effect on performance. Apparently, atomiz-

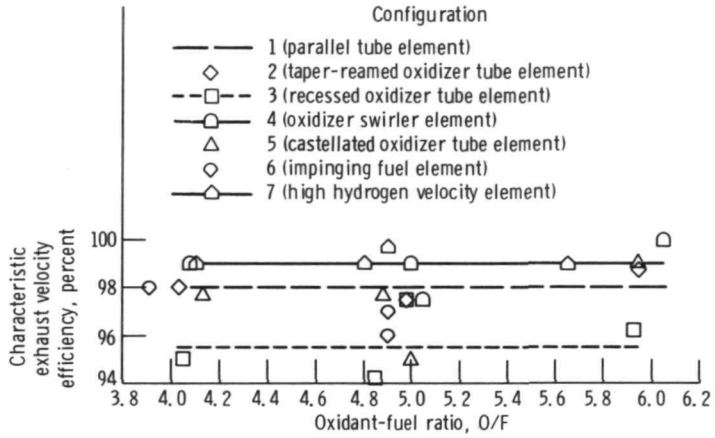

Figure 8. - Performance comparison of all element designs. Nominal chamber pressure, 3448 kilonewtons per square meter absolute (500 psia); nominal hydrogen injector inlet temperature, 33.3 K (60^0 R).

zation and mixing of the large diameter oxidizer jet was not enhanced by the higher velocity differential.

Configuration 3 (recessed oxidizer tube element). - The results of reference 2 indicated that an increase in performance was obtained with recessing of the oxidizer tube below the faceplate. Cold flow data (ref. 4) show maximum mixing efficiency of a coaxial tube element at a recess depth to jet diameter ratio of 1. For configuration 3, the oxidizer tube was recessed 0.508 centimeter (0.2 in.), slightly less in depth than the jet diameter. The oxidizer tube was taper-reamed similar to configuration 2.

The data in figure 8 show that the recessed element yielded combustion efficiencies that were about $2\frac{1}{2}$ percentage points lower than the flush element (configuration 2). This apparent disparity in test results between those of reference 2 and the present experiment is not understood.

Configuration 4 (oxidizer swirler element). - A technique, which has been used extensively with concentric tube elements to improve atomization and mixing of the center

oxidizer stream, was employed in configuration 4. Hydraulic swirlers were installed in all 19 otherwise baseline oxidizer elements as shown in figure 5(d). A comparison of spray characteristics with and without swirlers is shown in figure 9. The spray patterns were obtained with the elements flowing at design conditions and discharging into a pressurized environment of 1379 kilonewtons per square meter (200 psi). In the flow tests, water and gaseous nitrogen were used to simulate the oxidizer and fuel, respectively. The spray cone included angle increased from 2^{o} to 45^{o} with the addition of hydraulic swirlers. The effect of the improved atomization and mixing on combustion perperformance is seen in figure 8. The swirler element provided an improvement of about 1 percentage point in characteristic exhaust velocity compared to the conventional element. The oxidant injector pressure drop with the swirler element was about 345 kilonewtons per square meter (50 psi) higher than the conventional element.

Addition of swirlers appears to be an effective solution to improve performance,

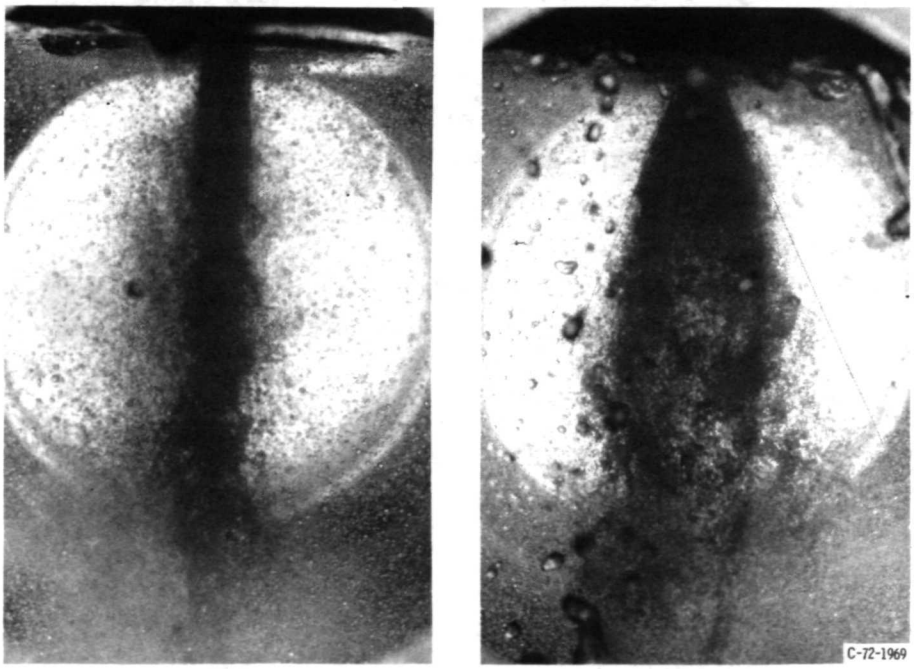

(a) Without swirler. (b) With swirler.

Figure 9. - Comparison of coaxial element characteristics using simulated propellants of water and gaseous nitrogen.

however, because of possible oxidizer wall impingement, a swirler element may not be desirable from the standpoint of ablative chamber compatibility. Configurations 5, 6, and 7 represent other attempts to improve atomization and mixing and yet remain compatible with ablative chambers and the use of film cooling.

Configuration 5 (castellated oxidizer tube element). - Another technique used in reference 1 to enhance atomization and mixing which had yielded an improvement in performance was castellating or slotting the end of the center oxidizer tube. This configuration was formed from the baseline configuration by machining six 0.23-centimeter- (0.090-in.-) wide by 0.508-centimeter- (0.200-in.-) deep radial slots in the end of the oxidizer tube (fig. 5(e)). The modification apparently did not significantly effect the atomization and mixing characteristics because no change in performance was observed compared to the baseline element. A marked effect, however, was noted on injector flow-pressure drop characteristics (shown in the section Injection Characteristics) with the modification. Also, some burning and metal discoloration of the oxidizer tube tip occurred indicating that the flame front had moved closer to the injector face.

Configuration 6 (impinging fuel element). - This element represents an attempt to enhance atomization and mixing of the center oxidizer jet by stream impingement. The fuel sleeves and oxidizer tube were modified such that the hydrogen sheet impinged on the oxygen jet at a half angle of 10°. The injection areas were the same as the baseline element. As seen in figure 8, the element yielded no improvement in performance over the baseline. Greater impingement angles may have been more effective. However, because a major injector modification would have been required to obtain a larger angle, such a change was not considered within the scope of this program.

Configuration 7 (high fuel velocity element). - Perhaps of only academic interest because of high pressure drop, the final configuration was designed to evaluate the effect of further increasing hydrogen injection velocity on performance. The total hydrogen injection area was reduced to 1.536 square centimeters (0.238 sq in.) compared to 2.075 square centimeters (0.322 sq in.) for the baseline element. At rated flow and a hydrogen injector inlet temperature of 33.3 K (60° R), the injection velocity was about 213 meters per second (700 ft/sec) and the injector pressure drop was 4480 kilonewtons per square meter (650 psi). The data again indicate the importance of hydrogen injection velocity on performance with concentric tube injectors. The high hydrogen velocity element yielded a characteristic exhaust velocity efficiency of 99 percent, about 1 percentage point higher than the baseline element (fig. 8).

In summary, these data indicate that very efficient combustion (η_{C^*} of 98 to 99 percent) can be achieved with large 2558-newton (575-lb) thrust per element injectors at hydrogen injector inlet temperatures of 33.3 K (60° R) by proper injector design. Several techniques to enhance atomization and mixing were tested, however, only installa-

tion of a swirler in the oxidizer tube or providing a high hydrogen injection velocity were successful in improving performance.

Injection Characteristics

As mentioned in the previous section, the design hydrogen injector differential pressure for the baseline element configuration 1 was as high as considered practical or about 1724 kilonewtons per square meter (250 psi) (0.5 of chamber pressure). The design oxidizer pressure drop was selected at about 0.3 of chamber pressure to provide good chugging stability.

The relation between propellant flow and injection differential pressure for all element designs tested are presented in figures 10 and 11. As expected, for an incompressible fluid, the oxygen flow varies as the square root of the differential pressure. The results show a slight increase of about 69 to 103 kilonewtons per square meter (10 to 15 psi) in oxidizer pressure drop due to recessing the tube 0.508 centimeter (0.2 in.) below the faceplate. The swirler element injector, as designed, had an oxidizer pressure drop of

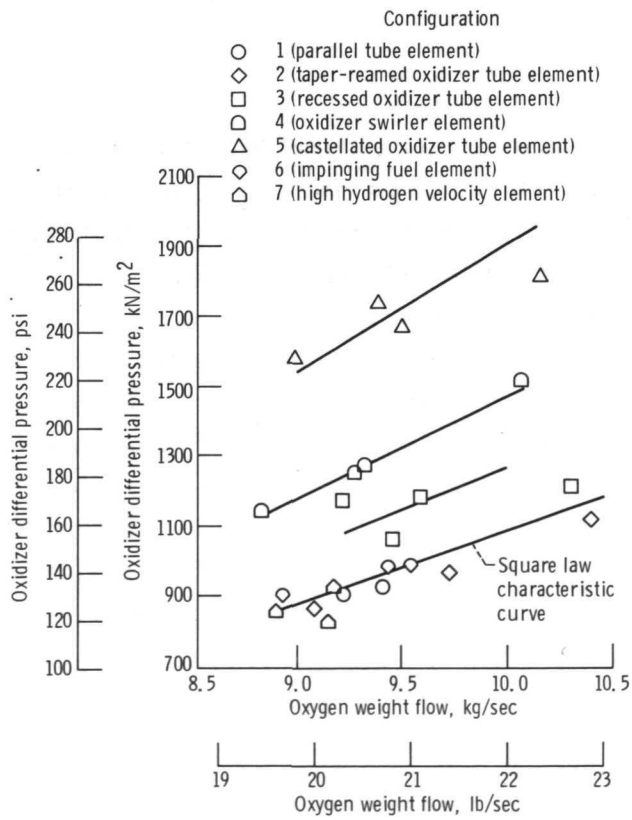

Figure 10. - Oxygen-injection flow characteristics.

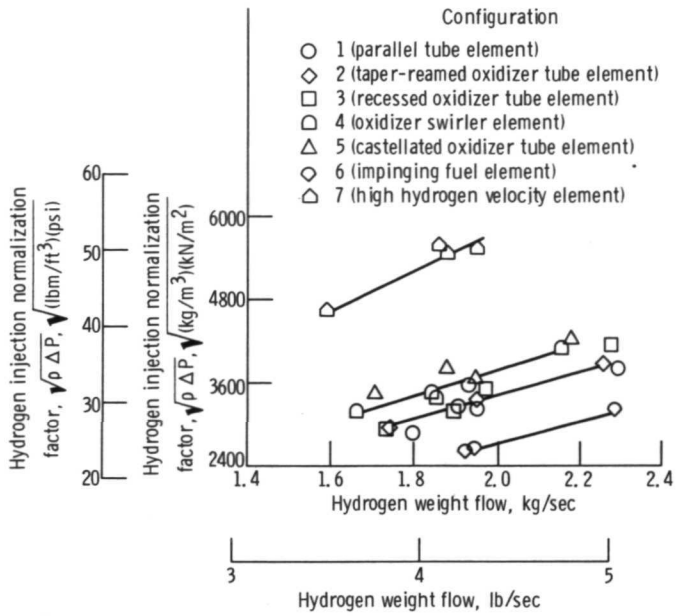

Figure 11. - Hydrogen-injection flow characteristics.

about 345 kilonewtons per square meter (50 psi) higher than the baseline element injector. The surprising result is the marked effect that castellating the element tip had on the flow characteristics. The pressure drop was approximately double that of the baseline element. This change is undoubtedly due to combustion at the exit of the oxidizer tube. As noted in the previous section, a postfiring inspection of the elements revealed overheating and a slight amount of metal erosion occurred during the tests.

Since hydrogen injector inlet temperature was not held precisely constant, the hydrogen-injection flow characteristics are presented as a function of a normalization factor (square root of the density times the differential pressure) in figure 11. With the exception of configuration 7, the high hydrogen injection velocity element, the hydrogen injection area was held constant and, as indicated by the data, modifications to the oxidizer tube had no strong effect on hydrogen pressure drop. Slight variations in pressure drop between configurations is believed to result from errors in hydrogen injector inlet temperature measurement and area variations due to machining tolerances.

In summary, with the exception of the castellated element injector, the hydraulic characteristics of the various designs were as expected. The design injector pressure drops provided injection velocities necessary for efficient combustion and also an adequate chugging and acoustic mode stability margin.

Injector-Ablative Chamber Compatibility

As mentioned in the INTRODUCTION, the ablative thrust chamber erosion characteristics were evaluated for two element configurations, the parallel tube element (configuration 1) and the oxidizer swirler element (configuration 4). The tests, however, included evaluating the effect of adding film cooling and varying the wall spacing between the outer row of elements and the wall on erosion rate.

All tests except one were conducted in thrust chambers assembled from paper reinforced phenolic rings (fig. 3). Each test chamber was subjected to a total firing duration of about 5 seconds made up of two $2\frac{1}{2}$-second-duration tests at an oxidant fuel ratio of 5 (nominal). The duration was limited to $2\frac{1}{2}$ seconds to prevent overheating of the uncooled injector faceplates. It should be noted that the erosion results presented in figures 12, 14, and 20 are average values and not the maximum depth at any given axial station. The average erosion depth was determined from cross-sectional area measurements obtained by planimetering tracings of the noncircular chamber circumference. An average circular diameter and thereby an average erosion depth was then computed assuming the measured flow area was circular.

Typical test results obtained with the parallel tube element injector without film cooling in a 13.68-centimeter- (5.39-in.-) diameter ablative chamber are shown in figure 12. Plotted is the average erosion depth as a function of axial chamber length. The erosion started at a length of about 7.62 centimeters (3 in.) from the injector and reached a maximum average depth of about 0.584 centimeter (0.23 in.) at a length of 20.3 centimeters (8 in.). The effect of installing oxidizer swirlers on erosion is also shown in figure 12. With swirlers, the erosion started immediately downstream of the

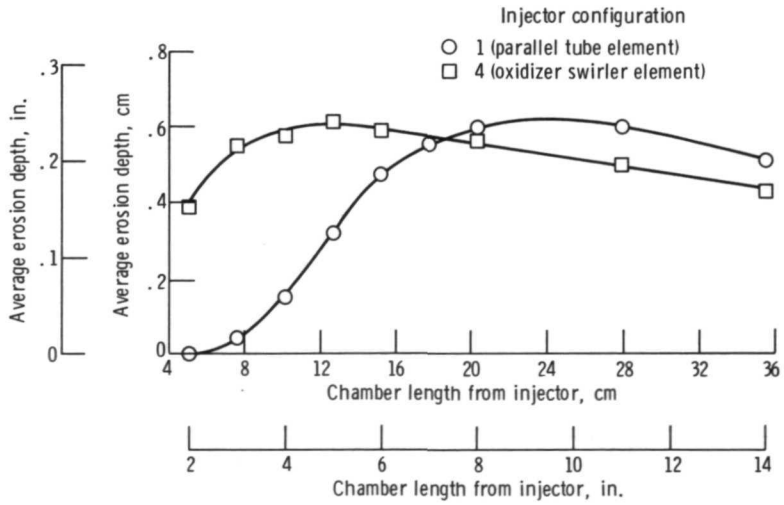

Figure 12. - Erosion characteristics of 19-element injector with and without oxidizer swirlers. Test duration, 5 seconds; chamber diameter, 13.68 centimeters (5.39 in.).

injector and reached the same maximum average depth of 0.584 centimeter (0.23 in.) but at a 12.7-centimeter (5-in.) length rather than 20.3 centimeters (8 in.). Shown in figure 13 are circumferential erosion patterns for the same injectors. The extreme gouging pattern was selected in each case. Without swirlers, maximum gouging adjacent to the element occurred at a length of 12.7 to 15.2 centimeters (5 to 6 in.) compared to 5.1 to 7.6 centimeters (2 to 3 in.) with swirlers. Note that maximum gouging did not occur at the same length as maximum average erosion. In both cases, the element gouging effect dissipated by 28 to 33 centimeters (11 to 13 in.) downstream and the circumferential erosion pattern became circular.

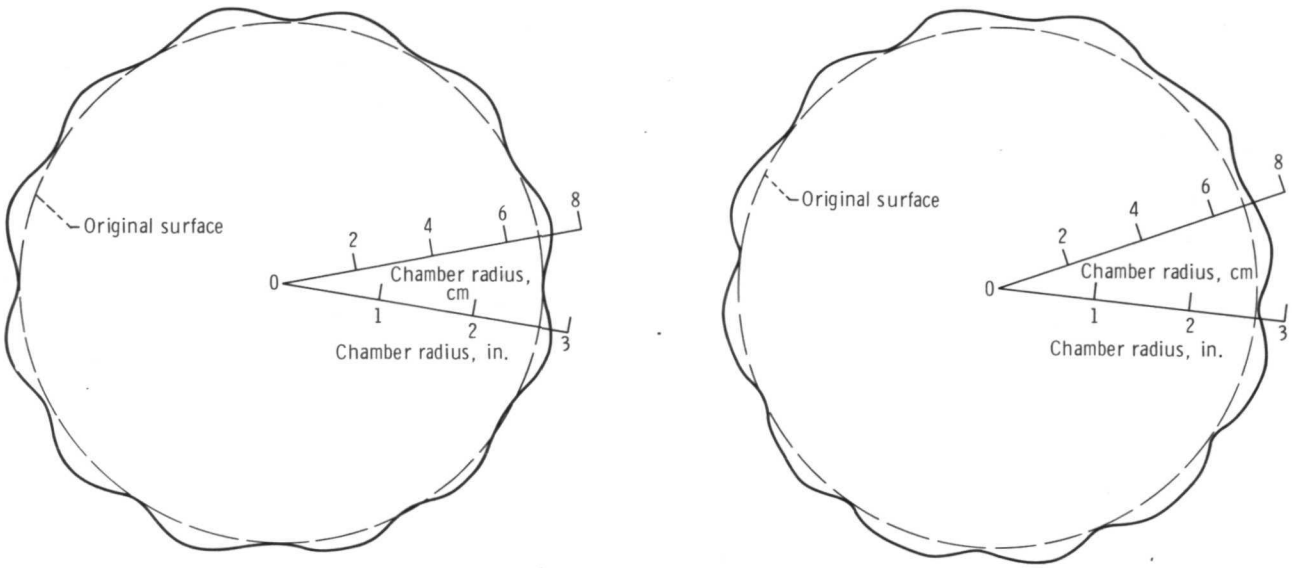

(a) Configuration 1 (parallel tube element); 12.7 centimeters (5 in.) downstream of injector.

(b) Configuration 4 (oxidizer swirler element); 5.08 centimeters (2 in.) downstream of injector.

Figure 13. - Circumferential erosion patterns for 19-element injector.

The ablative chamber durability with the swirler element injector could probably be improved by the technique of scarfing or cutting off the protruding oxidizer tube at an angle. This technique has been shown (ref. 5) to be effective in directing the injected propellant inward and, therefore, significantly reducing the heat transfer to the chamber walls.

Changing the spacing between the outer row of elements and the chamber wall also had considerable effect on ablative erosion near the injector. In figure 14 are plotted the results of tests using the swirler element injector in thrust chambers of 13.68 and 14.28 centimeters (5.39 and 5.62 in.) in diameter. The maximum average erosion depth decreased from 0.584 to 0.419 centimeter (0.23 to 0.165 in.) with the larger diameter chamber. Some of the decrease in average erosion resulted from a lesser

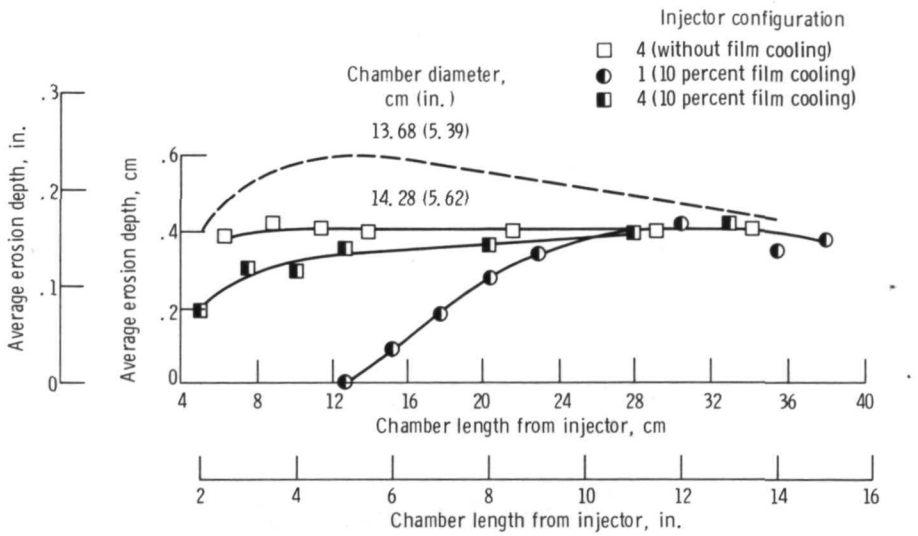

Figure 14. - Erosion characteristics of 19-element injector in 14.28-centimeter - (5.62-in. -) diameter chamber. Test duration, 5 seconds.

amount of gouging with the larger chamber. Also shown in figure 14 are some effects of film cooling on erosion for both injector configurations. The film cooling configuration consisted of 36 evenly spaced, 0.0914-centimeter- (0.036-in.-) diameter holes located on the faceplate at a diameter of 13.33 centimeters (5.25 in.). The holes were drilled such that every third hole was adjacent to an outer row injection element. The total film cooling flow area was 10 percent of the total hydrogen injection area. Examination of the results shows that film cooling significantly reduced the amount of erosion in the first 23 to 28 centimeters (9 to 11 in.) of the chamber for both injectors. At chamber lengths up to 12.7 centimeters (5 in.), film cooling prevented any erosion with the standard element and reduced the erosion by a third with the swirler injector. At 33 centimeters (13 in.), however, the erosion depth approached the other nonfilm cooled configurations indicating that the effectiveness had largely dissipated at this distance downstream. Combustion performance was not significantly degraded by the addition of 10 percent film cooling.

The addition of film cooling in the manner described did not alleviate the gouging of the ablative material adjacent to each outer injector element. In an attempt to reduce gouging, two tests were conducted to evaluate various film cooling hole patterns arranged to better cover the gouge areas. To minimize test cost, multiple film cooling hole patterns were drilled into the faceplate. One such faceplate is shown in figure 15. Patterns (120° segment) of one 0.158-centimeter (0.062-in.) hole, two 0.11-centimeter (0.043-in.) holes, and three 0.0914-centimeter (0.036-in.) holes were drilled adjacent to each outer row injector element. One additional faceplate was drilled with the same film cooling orifices but directed outward such that the film cooling jet would impinge

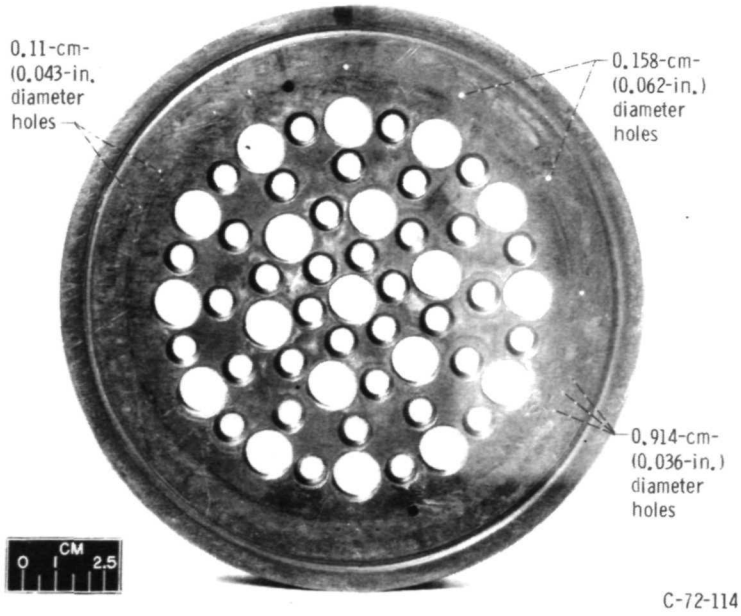

Figure 15. - Photograph of 19-element injector faceplate with three different film cooling hole patterns.

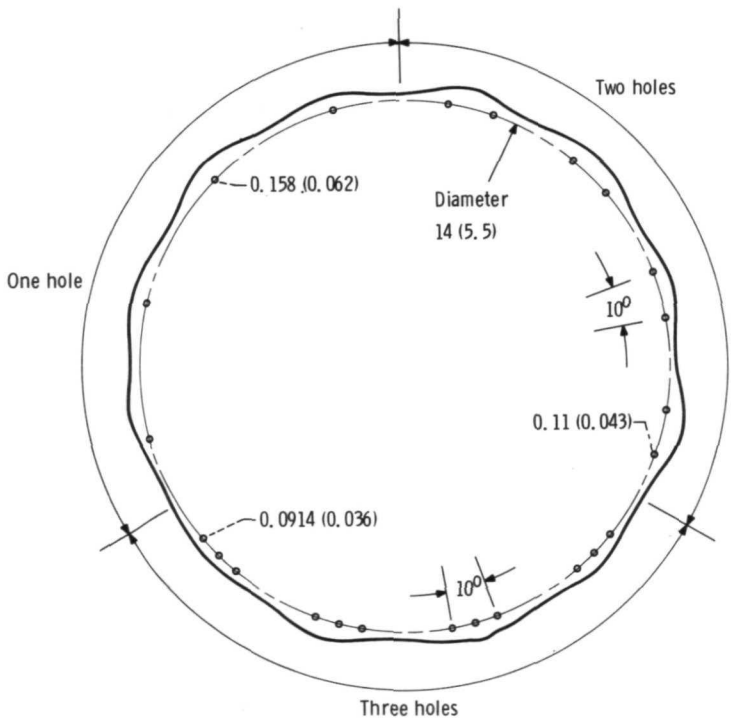

Figure 16. - Circumferential erosion patterns for 19-element (configuration 1) injector with three film cooling hole configurations; 17.8 centimeters (7-in.) from injector; ten percent film cooling. (All dimensions in cm (in.) unless indicated otherwise.)

upon the thrust chamber wall 5.08 centimeters (2 in.) downstream. The tests were conducted with parallel tube elements and at a 10-percent level of film cooling. A post-firing tracing of the thrust chamber cross section at an axial length of 17.8 centimeters (7 in.) is shown in figure 16. Examination of the figure shows that not any of the configurations (one, two, or three holes) eliminated the gouging problem. The three-hole pattern appeared to be the most effective of the film cooling patterns tested. Impinging the fuel onto the wall (not shown) did not improve its effectiveness.

The final test in the injector-thrust chamber ablative compatibility series consisted of a 20-second-duration firing at an oxidant-fuel ratio of 5 with a 13.68-centimeter- (5.39-in.-) diameter and 74.4-centimeter- (29.3-in.-) long, high purity silica, phenolic ablative chamber with good ablative characteristics. A sketch of the thrust chamber liner is shown in figure 17. The ablative material was composed of 70 percent silica reinforcement and manufactured to Fiberite specificiation MX-2641. The reinforcement was 1.27- by 1.27-centimeter (1/2- by 1/2-in.) chopped square silica cloth. The parallel tube element (configuration 1) injector but with a transpiration-cooled faceplate drilled with the three-hole (0.0914 cm (0.036 in.) diam.) 10-percent film cooling pattern (fig. 18) was used for the tests. The axial and circumferential erosion is shown

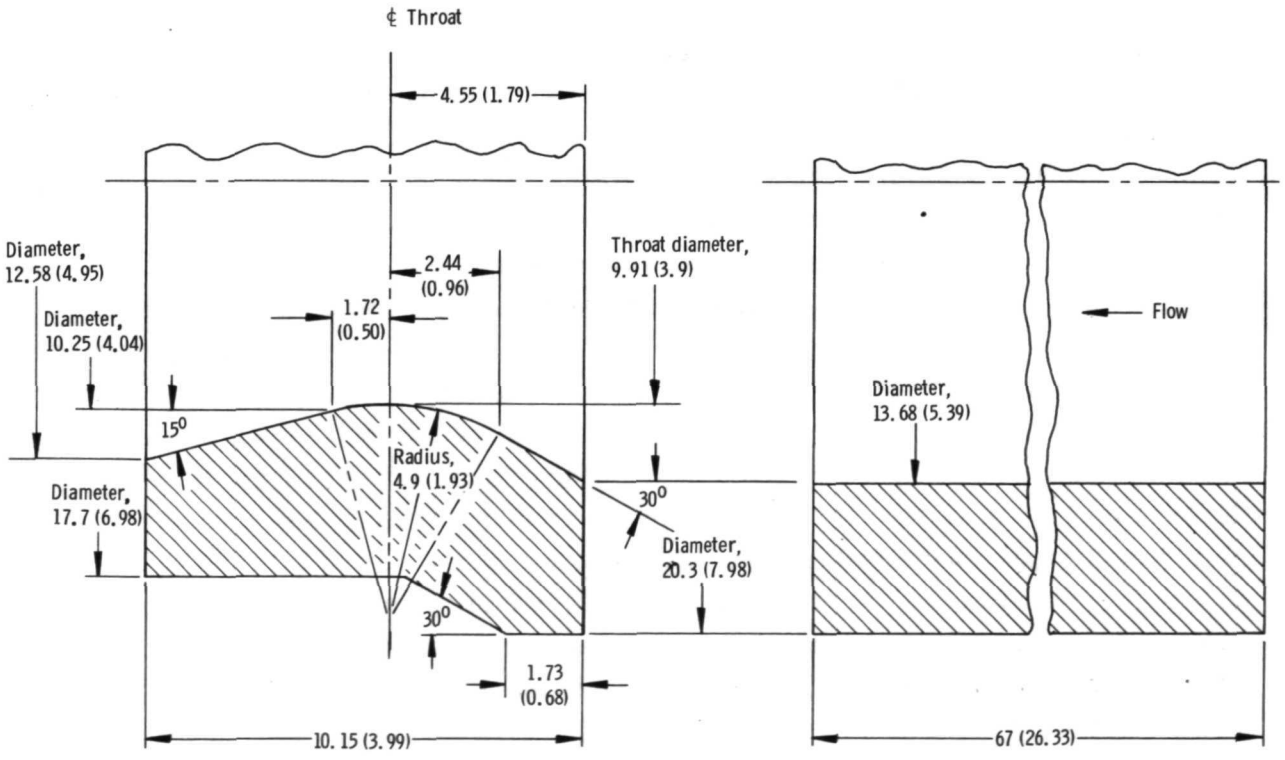

Figure 17. - Cross-sectional view of high purity silica, phenolic chamber. (All dimensions in cm (in.) unless indicated otherwise.)

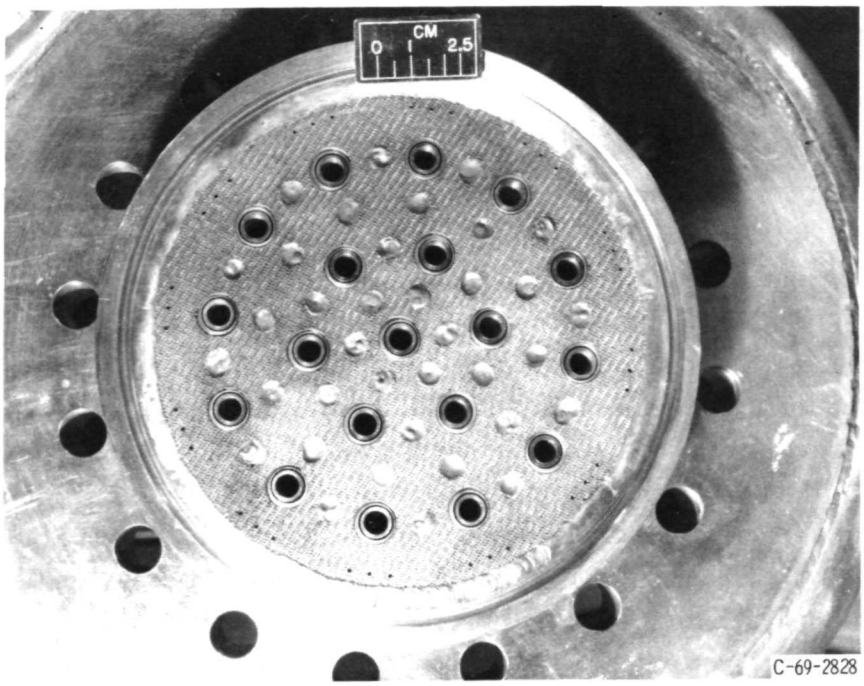

Figure 18. - Photograph of 19-element injector with transpiration cooled faceplate and three-hole film cooling configuration.

in figures 19 and 20. Examination of figure 19, which is a cross-sectional view of the ablative chamber 24.4 centimeters (9.6 in.) downstream, shows a slight amount of gouging from each outer injection element. Also, the char layer was not of uniform thickness around the circumference. The average erosion depth axially down the chamber is shown in figure 20. In the cylindrical section or to an axial length of about 69.6 centimeters (27.4 in.), the results indicate a negative change. This phenomena is not unusual and has been observed by many investigators. The behavior is associated with the firing duration. During the first part of a firing, the chamber inside diameter decreases because of roughening of the surface and swelling of material during the process of charring. After this period, the ablative material erodes quite linearly with firing time as shown in reference 6. At the throat of the thrust chamber (axial length of 74.4 cm or 29.3 in.), the average ablative erosion depth was 0.414 centimeter (0.163 in.) for the 20-second firing or an average erosion rate of 0.0208 centimeter per second (0.0082 in./sec). In subscale tests of M-1 injector elements (ref. 7), the average erosion rate varied from 0.013 to 0.036 centimeter per second (0.0051 to 0.0142 in./sec) for a similar high purity silica phenolic ablative.

In summary, protection of the ablative chamber from gouging appears to be a problem area with large thrust per element injectors. Film cooling up to a 10-percent level did not eliminate the gouging problem near the injector. The problem could possibly be alleviated with higher film cooling rates, however, higher rates may result in a per-

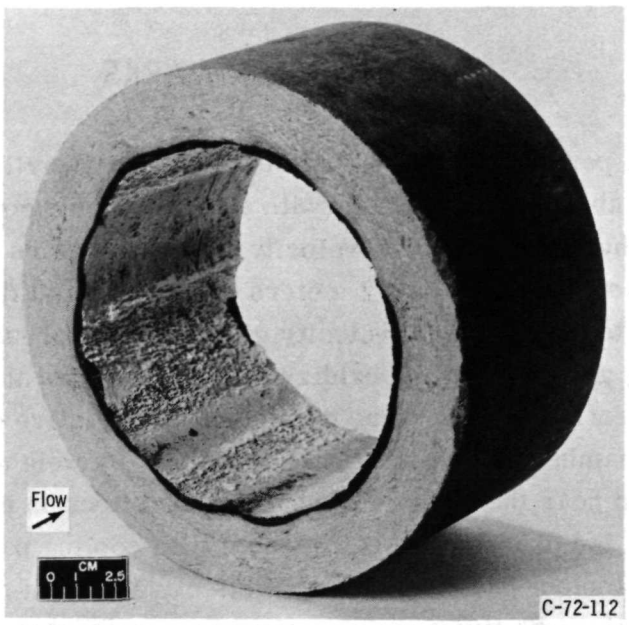

Figure 19. - Cross-sectional view of ablative thrust chamber 24.4 centimeters (9.6 in.) downstream of injector. Firing duration, 20 seconds.

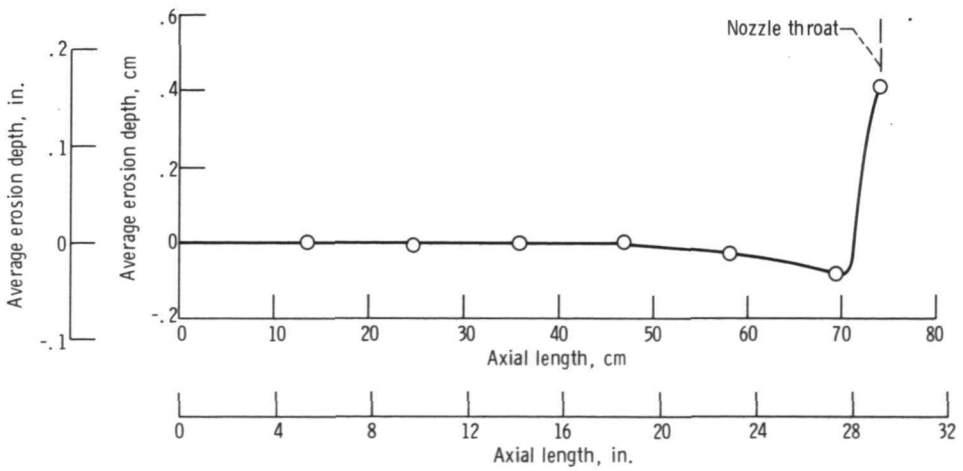

Figure 20. - Erosion of high silica content ablative thrust chamber in a 20-second firing duration; 19-element injector with configuration 1 elements and 10 percent film cooling.

formance penalty. Perhaps oxidant-fuel zone cooling or an injector with an outer row of smaller injection elements would provide an environment more compatible with the ablative chamber.

CONCLUDING REMARKS

High combustion performance was obtained with relatively large elements at hydrogen temperatures of about 33.3 K (60° R) with a parallel tube coaxial injector. An element designed for a hydrogen injection velocity of 158.5 meters per second (520 ft/sec) and an oxygen injection velocity of 12.2 meters per second (40 ft/sec) yielded 98 percent of theoretical characteristic exhaust velocity efficiency. Increasing hydrogen injection velocity or providing a swirler in the oxidizer tube, improved the combustion performance by about 1 percent. Swirlers were detrimental to ablative compatibility near the injector end of the chamber. Film cooling, 10 percent by weight, significantly reduced the amount of erosion near the injector, but had little effect on erosion at 33 centimeters (13 in.) down the chamber. A three-hole film cooling pattern adjacent to each outer row injection element provided the most effective coolant distribution from the standpoint of eliminating ablative gouging. However, none of the hole sizes or patterns completely eliminated the gouging adjacent to each outer injection element.

Lewis Research Center,
National Aeronautics and Space Administration,
Cleveland, Ohio, May 19, 1972,
113-31.

APPENDIX A

CHARACTERISTIC EXHAUST VELOCITY EFFICIENCY

Characteristic exhaust velocity efficiency is calculated in the following manner (Symbols are defined in appendix B.):

$$\eta_{C^*} = \frac{C^*_{exp}}{C^*_{th}}$$

where C^*_{th} is from reference 3 and

$$C^*_{exp} = \frac{P_c A_t g}{\dot{W}}$$

$$P_c = \frac{P_{inj}}{MPL}$$

$$MPL = \frac{P_1}{P_c} + \frac{I_1 g - V_{avg}}{C^*_{th} \epsilon}$$

$$V_{avg} = \frac{V_{H_2} \dot{W}_{H_2} + V_{O_2} \dot{W}_{O_2}}{\dot{W}}$$

APPENDIX B

SYMBOLS

A_{ch}	area of chamber, cm^2; $in.^2$
A_t	area of throat, cm^2, $in.^2$
C^*_{exp}	experimental characteristic exhaust velocity, m/sec; ft/sec
C^*_{th}	theoretical characteristic exhaust velocity (ref. 3), m/sec; ft/sec
g	gravitational conversion factor, kg-m/N-sec^2; (lb m-ft)/(lb f-sec^2)
I_1	theoretical specific impulse at nozzle inlet (ref. 3), N-sec/kg; lb f-sec/lb m
MPL	momentum pressure loss
ΔP	hydrogen-injection differential pressure, kN/m^2; psi
P_c	total pressure in nozzle, kN/m^2 abs; psia
P_{inj}	chamber pressure at injector face kN/m^2 abs; psia
P_1	static pressure at nozzle inlet, kN/m^2 abs, psia
V_{avg}	average injection velocity, m/sec; ft/sec
V_{H_2}	hydrogen-injection velocity, m/sec; ft/sec
V_{O_2}	oxygen-injection velocity, m/sec; ft/sec
$\dot{W}$	propellant weight flow, kg/sec; lb m/sec
$\dot{W}_{H_2}$	hydrogen weight flow, kg/sec; lb m/sec
$\dot{W}_{O_2}$	oxygen weight flow, kg/sec; lb m/sec
ϵ	contraction ratio, A_{ch}/A_t
η_{C^*}	characteristic exhaust velocity efficiency, percent
ρ	hydrogen density, kg/m^3; lb m/ft^3

REFERENCES

1. Hannum, Ned P.; and Conrad, E. William: Performance and Screech Characteristics of a Series of 2500-Pound Thrust-per-Element Injectors for a Liquid-Oxygen-Hydrogen Rocket Engine. NASA TM X-1253, 1966.

2. Wanhainen, John P.; Parish, Harold C.; and Conrad, E. William: Effect of Propellant Injection Velocity on Screech in 20,000-Pound Hydrogen-Oxygen Rocket Engine. NASA TN D-3373, 1966.

3. Sievers, Gilbert K.; Tomazic, William A.; and Kinney, George R.: Theoretical Performance of Hydrogen-Oxygen Rocket Thrust Chambers. NASA TR R-111, 1961.

4. Burick, R. J.: Space Storable Propellant Performance. Rocketdyne. NASA CR-120936, 1972.

5. Anon.: Space Storable Regenerative Cooling Investigation. Rep. PWA-FR-4000, Pratt & Whitney Aircraft (NASA CR-72704), Oct. 8, 1971.

6. Pavli, A. J.: Experimental Evaluation of Several Advanced Ablative Materials as Nozzle Sections of a Storable-Propellant Rocket Engine. NASA TM X-1559, 1968.

7. Dankhoff, Walter F.; Johnsen, Irving A.; Conrad, E. William; and Tomazic, William A.: M-1 Injector Development-Philosophy and Implementation. NASA TN D-4730, 1968.

NASA-Langley, 1972 —— 33 E-6926